

Order–disorder transition in monoclinic sulfur: a precise structural study by high-resolution neutron powder diffraction.

Corrigendum

W. I. F. David,^a R. M. Ibberson,^{a*} S. F. J. Cox^a and P. T. Wood^{b‡}

^aISIS Facility, CCLRC, Rutherford Appleton Laboratory, Chilton, Didcot, Oxfordshire OX11 0QX, England, and ^bSchool of Chemical Sciences, University of East Anglia, Norwich, Norfolk NR4 7TJ, England

‡ Present address: The University Chemical Laboratory, University of Cambridge, Lensfield Road, Cambridge CB2 1EW, England.
Correspondence e-mail: r.m.ibberson@rl.ac.uk

Revised lattice parameters for Table 1 of the paper by David *et al.* (2006), *Acta Cryst. B* **62**, 953–959, are given.

The lattice constants for β -sulfur at 100 K given in Table 1 of the paper by David *et al.* (2006) are incorrect. Correct values are: $a = 10.8027(1)$, $b = 10.6911(1)$, $c = 10.6689(1)$ Å; $\beta = 95.7124(10)^\circ$; $V = 1226.06(2)$ Å³. Also, the a and c axis labels shown in Fig. 2(a) should be reversed.

References

David, W. I. F., Ibberson, R. M., Cox, S. F. J. & Wood, P. T. (2006). *Acta Cryst. B* **62**, 953–959.

Order–disorder transition in monoclinic sulfur: a precise structural study by high-resolution neutron powder diffraction

W. I. F. David,^a R. M. Ibberson,^{a*}
S. F. J. Cox^a and P. T. Wood^{b‡}

^aISIS Facility, CCLRC, Rutherford Appleton Laboratory, Chilton, Didcot, Oxfordshire OX11 0QX, England, and ^bSchool of Chemical Sciences, University of East Anglia, Norwich, Norfolk NR4 7TJ, England

‡ Present address: The University Chemical Laboratory, University of Cambridge, Lensfield Road, Cambridge CB2 1EW, England.

Correspondence e-mail: r.m.ibberson@rl.ac.uk

High-resolution neutron powder diffraction has been used in order to characterize the order–disorder transition in monoclinic cyclo-octasulphur. Rapid data collection and the novel use of geometrically constrained refinements has enabled a direct and precise determination of the order parameter, based on molecular site occupancies, to be made. The transition is critical and continuous; with a transition temperature, $T_c = 198.4(3)$ K, and a critical exponent, $\beta = 0.28(3)$, which is indicative of three-dimensional ordering. Difficulties encountered as a consequence of the low thermal conductivity of the sample are discussed.

Received 3 February 2006
Accepted 25 September 2006

1. Introduction

Sulfur is one of the few elements that possesses multiple allotropes and associated structural phase transitions (see, for example, Meyer, 1976; Donahue, 1982). The rich structural variety of cyclo-octasulphur provides case studies for the analysis of a number of general phenomena that include allotrope comparison and reaction kinetics, pre-melting behaviour, premonitory reconstructive phase-transition effects, the modelling of static and dynamic disorder, critical behaviour and anomalous thermal expansion. The complex phase diagram of elemental sulfur also provides an attractive testing ground for theoretical studies and has been the subject of recent molecular dynamics simulations (Pastorino & Gamba, 2001, 2003).

At ambient temperature the stable form of S_8 is α -sulfur, also known as (ortho)rhombic sulfur or Muthmann's sulfur – space group $Fddd$, $a = 10.4646$, $b = 12.8660$, $c = 24.4859$ Å, $Z = 16$ (Pawley & Rinaldi, 1972; Coppens *et al.*, 1977; Rettig & Trotter, 1987). Above 368 K, α -sulfur converts to β -sulfur, also known as monoclinic sulfur – space group $P2_1/a$, $a = 10.778$, $b = 10.844$, $c = 10.924$ Å, $\beta = 95.80^\circ$, $Z = 6$ (Sands, 1965; Templeton *et al.*, 1976), which in turn melts at 392 K (see Fig. 1). Whereas α -sulfur is ordered at all temperatures, high-temperature β -sulfur is partially ordered with one-third of the non-centrosymmetric crown-configuration S_8 molecules possessing one of two orientations, which adds $(R/3)\ln 2$ to the entropy per mole

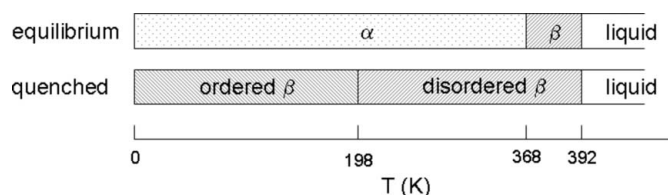


Figure 1
The phase diagram for α - and β -sulfur.

Table 1

Experimental details for β -sulfur at 100 K.

| | |
|--|--|
| Crystal data | |
| Chemical formula | S ₈ |
| M_r | 256.58 |
| Cell setting, space group | Monoclinic, $P2_1$ |
| Temperature (K) | 100 |
| a, b, c (Å) | 10.8125 (1), 10.7232 (1), 10.6883 (1) |
| β (°) | 95.7460 (10) |
| V (Å ³) | 1233.02 (2) |
| Z | 6 |
| D_x (Mg m ⁻³) | 2.073 (1) |
| Radiation type | Time-of-flight neutron |
| Specimen form, colour | Flat sheet (particle morphology: irregular powder), yellow |
| Specimen size (mm) | 20 × 15 × 15 |
| Data collection | |
| Diffractometer | HRPD |
| Data collection method | Specimen mounting: standard rectangular sample holder (vanadium windows); time-of-flight range 45–145 ms |
| Total flight path (m), $\langle 2\theta \rangle$ (°) | 95.89, 168.329 |
| Refinement | |
| Refinement on | Rietveld method |
| R -factors and goodness-of-fit | $R_p = 0.049$, $R_{wp} = 0.053$, $R_{exp} = 0.030$, $R_B = 0.069$, $S = 3.19$ |
| Wavelength of incident radiation (Å) | 1.85–5.98 |
| Excluded region(s) | None |
| Profile function | CCSL TOF profile function |
| No. of parameters | 86 |
| Weighting scheme | Based on measured s.u.s |
| $(\Delta/\sigma)_{max}$ | 0.04 |

Computer programs used: ISIS Instrument control program (ICP), *TF12LS* (David *et al.*, 1992), standard HRPD normalization routines, *PLATON* (Spek, 2003).

of S₈ (Sands, 1965). Heat-capacity measurements (Montgomery, 1974) show that this entropy is lost at a critical continuous λ transition at 198 K so that the thermodynamically stable states of both α -sulfur and β -sulfur at absolute zero are fully ordered. The most recent structural paper on β -sulfur by Goldsmith & Strouse (1977) has confirmed, using single-crystal X-ray diffraction, that the transition is continuous and most likely to follow a three-dimensional Ising Model behaviour. However, their evidence is incomplete since they were only able to perform full structural analyses at five temperatures (13, 143, 198 and 218 K) and no direct measurement of the order parameter could be made.

Using high-resolution neutron powder diffraction, we have been able to fully characterize the order–disorder transition in monoclinic sulfur. This requires a high resolution for accurate lattice-parameter measurement, high- Q data for accurate positional, thermal and site occupancy measurements, precise temperature control and rapid measurement. Although the compound is a single element and apparently equally suited to X-ray diffraction, our experience from C₆₀ (David *et al.*, 1993) shows that neutron powder diffraction is particularly appropriate as a rapid and precise technique for structural surveying.

2. Experimental

2.1. Sample preparation

Sulfur flakes (Aldrich Chemical Co.) were hand ground and *ca* 6 cm³ of the resulting fine powder then sealed under helium gas in a rectangular sample can. The sample-can body was fabricated from aluminium alloy and incorporated a heater and Rh/Fe sensor; the sample was irradiated by the neutron beam through thin vanadium windows. Monoclinic sulfur was prepared by heating the sample to 380 K inside a standard ‘orange’ He-flow cryostat maintained at 200 K. At room temperature, the transformation from β - to α -sulfur takes less than 1 h, although below 250 K β -sulfur is stable for several weeks. However, attempts to quench the sample in the β phase within the cryostat using a cooling rate of some 20 K min⁻¹ proved unsuccessful. Removing the sample from the cryostat and then quenching in liquid nitrogen yielded a phase-pure sample of monoclinic sulfur.

2.2. Data collection

The sample was removed from liquid nitrogen and mounted on a displacer before cooling to 40 K. During the transfer period, at no time did the sample temperature exceed 240 K. Time-of-flight neutron powder diffraction data were collected on the high-resolution powder diffractometer (HRPD; Ibberson *et al.*, 1992) at the ISIS pulsed neutron source. Data were recorded at backscattering, $\langle 2\theta \rangle = 168$, over a time-of-flight range between 45 and 145 ms, corresponding to a d -spacing range of between 0.9 and 2.9 Å. Under these experimental settings the instrumental resolution, $\Delta d/d$, is approximately constant and equal to 8×10^{-4} .

Diffraction data were recorded at 5 K intervals between 40 and 175 K, and between 215 and 250 K for a period of approximately 25 min (18 μ Ah); at each 25 K interval (*i.e.* at 50, 75, 100 K *etc.*) a longer data collection period, 140 min (100 μ Ah), was used. Over the region of the λ transition, between 180 and 210 K, data were also recorded at 2 K intervals for 18 μ Ah. In all cases, a period of 5 min for temperature equilibration was allowed between each data set.

2.3. Data analysis

A standard data reduction procedure was followed: the data were normalized to the incident-beam monitor profile and corrected for detector-efficiency effects using a previously recorded vanadium spectrum. The diffraction data were analysed using an in-house program suite adapted for neutron time-of-flight data (David *et al.*, 1992) and based on the Rietveld method. The peak shape used in the refinement was the standard form for the high-resolution powder diffractometer (HRPD) at ISIS consisting of the convolution of a Voigt function with a double-exponential decay. Experimental details are given in Table 1.¹

¹ Supplementary data for this paper are available from the IUCr electronic archives (Reference: WS5045). Services for accessing these data are described at the back of the journal.

Table 2

Average intermolecular bond lengths (Å) and angles (°).

| | Neutron powder diffraction (this work) 100 K | X-ray single-crystal diffraction (113 K)† |
|---------------------------|--|--|
| (S–S) _I (Å)‡ | 2.052 (10) | 2.051 (2) |
| (S–S) _{II} (Å)‡ | 2.052 (10) | 2.049 (2) |
| (S–S) _{III} (Å)‡ | 2.052 (10) | 2.02 (3) |
| (S–S) _I (°)‡ | 107.4 (5) | 107.66 (6) |
| (S–S) _{II} (°)‡ | 107.4 (5) | 108.10 (6) |
| (S–S) _{III} (°)‡ | 107.4 (5) | 114 (1) |

† See Goldsmith & Strouse (1977). ‡ Molecule (I) comprises atoms S1–S8, molecule (II) atoms S9–S16 and the disordered molecule (III) atoms S17–S24 and S17'–S24'.

Atomic positions for the initial model of the ordered structure were taken from the 113 K data of Goldsmith & Strouse (1977). As was the case with the single-crystal X-ray study, the refinements were performed in the space group $P2_1$ with the 2_1 axis at $x = 0$, $z = \frac{1}{2}$, and with the constraint that the site occupancies for the disordered pseudocentric molecules summed to one. Although only a single parameter was refined for the fractional occupancy of one of the molecular sites, the structural analysis remained complex even with high-resolution powder diffraction data since there are four molecules, two ordered and the pseudocentric disordered pair, in the asymmetric unit and thus over 90 refinable parameters in terms of atomic coordinates alone. Indeed the comparatively weak neutron scattering length of sulfur ($b = 2.847$ fm) along with pseudosymmetry in the lattice-parameter values contribute additional difficulties with the analysis, especially with the rapidly collected data. It was therefore necessary to impose additional constraints on the structural model.

Firstly, the pseudocentricity of the disordered S_8 crowns was rigorously imposed and the isotropic displacement parameters on the two ordered molecules were constrained to be

equal, as were those of the partially occupied disordered molecular sites. Second, geometric bond length and angle constraints were applied. The bond lengths and angles were divided into two sets corresponding to the ordered and disordered molecules; in each set the bond lengths and angles were weakly restrained to be equal within ± 0.001 Å and $\pm 0.01^\circ$, respectively. These restraints are consistent with results from the single-crystal X-ray refinements (Goldsmith & Strouse, 1977) and have the advantage of biasing the refinement towards a chemically reasonable result, but without dictating precise bond-length and bond-angle values. A scale factor, coefficients of a background polynomial function, lattice constants and sample-dependent peak-width parameters were also refined.

3. Results and discussion

3.1. Structure refinement

The structure of monoclinic sulfur is illustrated in Fig. 2 and the result of the profile fitting to the 100 K data set is shown in Fig. 3. The complexity of the powder diffraction pattern is evident. Table 2 lists the average bond lengths and bond angles for the ordered and disordered S_8 molecules in the structure in comparison with the 113 K X-ray single-crystal refinement. The values from the neutron powder data of 2.052 (10) Å and 107.4 (3)° for the average intramolecular bond length and bond angle, respectively, are in excellent agreement with the single-crystal values. Again, it should be emphasized that the constraints during refinement are only for equivalence between bond lengths and angles with no specific value being assigned. The method is further validated in that slight deviations from the ideal crown configuration observed in the single-crystal study are not significant compared with the estimated standard deviations on the bond length and angle values in the present study. The estimated standard

deviations are some 3–5 times greater in the neutron-powder study than in the X-ray single-crystal study.

3.2. Order–disorder transition

3.2.1. Bragg–Williams model. The crystal structure of monoclinic sulfur showing the two pseudocentric orientations is illustrated in Fig. 2. It is the intermolecular interactions between neighbouring symmetry-related molecules which are responsible for the energy difference between the two orientations. Gold-

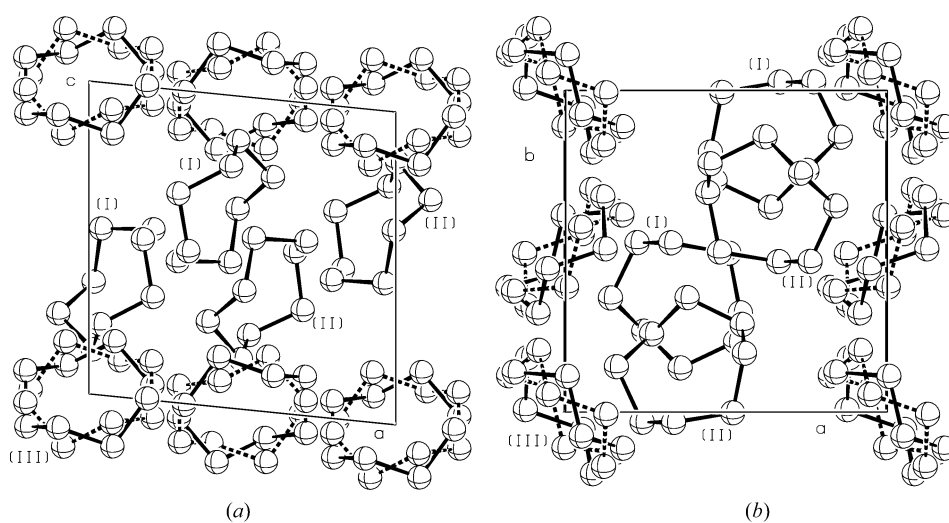
**Figure 2**

Illustration of the crystal structure of monoclinic sulfur, viewed (a) along the b axis and (b) along the c axis. The three S_8 molecules in the asymmetric unit are denoted as (I) (atoms S1–S8), (II) (atoms S9–S16) and the disordered molecule (III) (atoms S17–S24, S17'–S24').

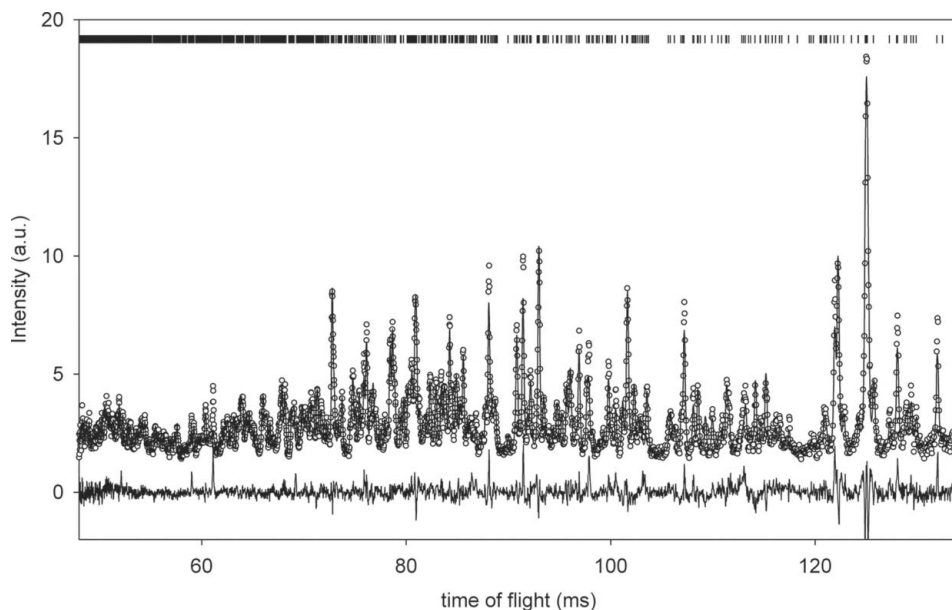


Figure 3
Observed (circle), calculated (line) and difference/e.s.d profiles for monoclinic sulfur at 100 K. The vertical tick marks represent the calculated peak positions.

smith & Strouse (1977) recognized that this dependency on the orientation of neighbouring molecules requires that the order–disorder transition be cooperative and used a simple Bragg–Williams model to characterize the transition using the limited information available.

The Bragg–Williams model of cooperative order–disorder transitions is typically applied in the description of transitions of alloys (see, for example, Muto & Takagi, 1955) and magnetic spin $\frac{1}{2}$ systems (see, for example, Collins, 1989). It is a self-consistent model in which the energy of the system is expressed in terms of a long-range order parameter P , which corresponds to the difference in the fractional occupations of

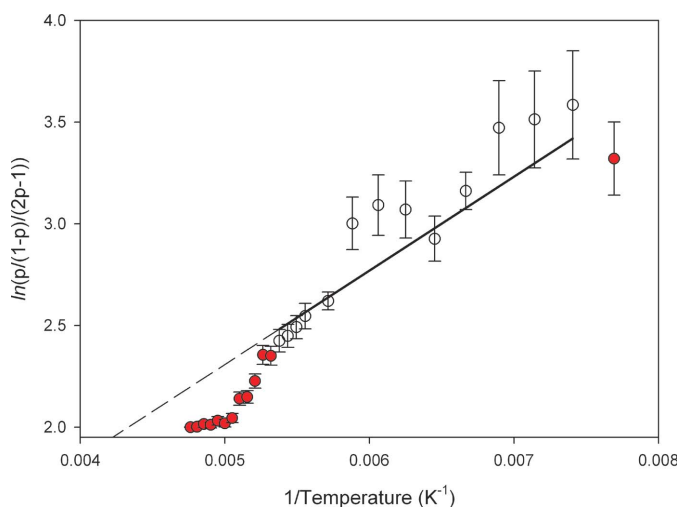


Figure 4
The temperature dependence of the long-range order parameter, P , based on the Bragg–Williams model. The ordering energy, $U = 462$ (4) K, is determined by a least-squares fit to the points indicated (open circles).

the two sites and an ordering energy U , which corresponds to the difference in energy between the two sites in the otherwise ordered structure. The temperature dependence of P based on the Bragg–Williams model is as follows

$$\frac{R \ln\left(\frac{1+P}{1-P}\right)}{P} = \frac{U}{T}. \quad (1)$$

Fig. 4 shows a fit to the data using this expression. The model dictates that below the critical temperature, $\ln[(1+P)/(1-P)/P]$ versus $1/T$ be linear with a slope of U/R . The transition temperature, T_c , is defined simply as half the value of the ordering energy, U . As the critical temperature is approached, the data clearly deviate from the Bragg–Williams limit. This is not surprising since the model neglects the effects of short-range order and the variation of U owing to the

temperature dependence of the lattice parameters. Thus, the refined value of U of 462 (4) K may be regarded simply as an indication of the magnitude of the ordering energy of the system. Goldsmith & Strouse (1977) derived a value of U of 553 K using a similar approach, which is comparable to the present study although based on just two measurements below the transition temperature. The temperature dependence of the observed disorder is best analysed in terms of mean-field behaviour, as described below.

3.2.2. Mean-field model. The X-ray single-crystal data recorded at only five different temperatures by Goldsmith &

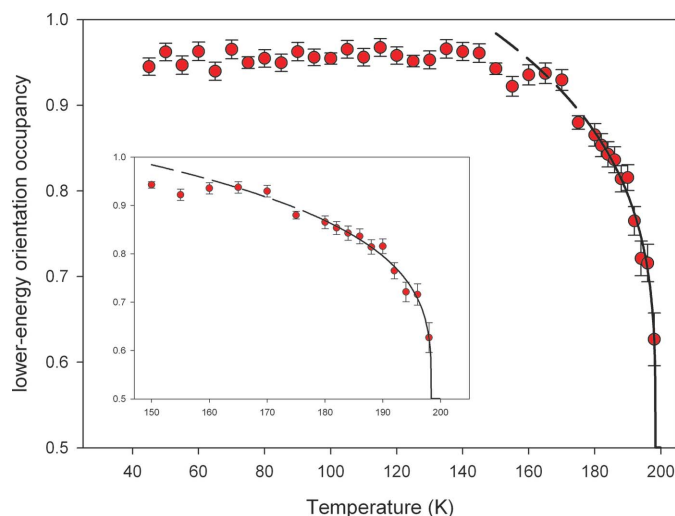


Figure 5
Power-law behaviour of the refined values of the lower-energy orientation site occupancy: inset shows the range $150 < T < 200$ K. The solid line is the least-squares fit to the points above 180 K. Saturation effects below 150 K are clearly seen.

Strouse (1977) are not sufficient for quantitative analysis of the critical behaviour associated with the transition. However an indirect estimate of the order parameter was made by measuring the variation of intensity of the (503) reflection as a function of temperature. Least-squares fitting of 54 measure-

ments between 178 and 196 K for T_c between 197 and 198 K gave a value for the critical exponent β of between 0.27 and 0.33. The standard deviations of the critical exponents were in the range 0.003–0.005, however, a precise determination of the critical temperature was not possible since near T_c both Bragg and critical scattering make significant contributions to the observed intensity. The refined site occupancies as determined from the present neutron powder diffraction study are shown in Fig. 5. Below the critical temperature the occupancy of the lower energy orientation (n_{lower}) can be fitted assuming power law behaviour of the form

$$n_{\text{lower}} = 0.5 + \alpha(1 - T/T_c)^\beta \quad (2)$$

The good quality of the fit is evident from Fig. 5 and gives a value for the critical exponent, β , of 0.28 (3) and $T_c = 198.4$ (3) K, which is in excellent agreement with the value of 198 K determined by heat-capacity measurements (Montgomery, 1974). A value of β in the region of 0.3 indicates short-range three-dimensional Ising Model behaviour indicative of dipole–dipole or, more likely, van der Waals interactions. Whilst the region just below T_c is well modelled, below 150 K saturation of the critical behaviour is clearly evident.

3.3. Lattice parameter variation

The refined values of the lattice parameters of monoclinic sulfur between 40 and 250 K are shown in Fig. 6. In each case the 198 K transition is evident and a smooth variation of the lattice parameters is observed across the region of the transition. There are a number of other notable features. In particular, the behaviour of the monoclinic β angle is anomalous and shows premonitory effects, apparently coincident with the saturation of the site occupancy, above 150 K. The most marked change in the unit-cell edges associated with the transition is along **a** and this is consistent with the molecular packing of the three molecules in the asymmetric unit. Along

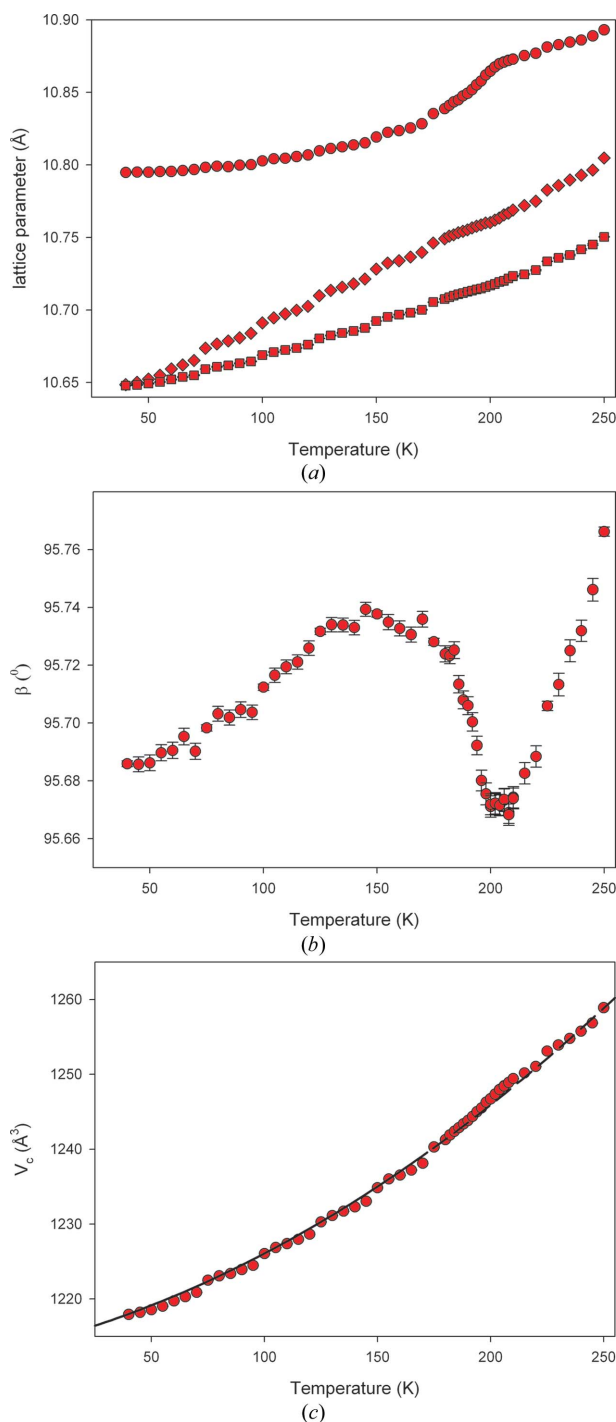


Figure 6 Variation of the lattice constants of β -sulfur with temperature: (a) *a* (circle), *b* (diamond) and *c* (square) lattice constants; (b) monoclinic β angle; (c) unit-cell volume. The unit-cell data from the long count-time runs at 40, 75, 100, 125, 150 and 175 K are fitted to a quadratic function shown by a solid line. The extrapolated fit above 175 K is shown by a dashed line.

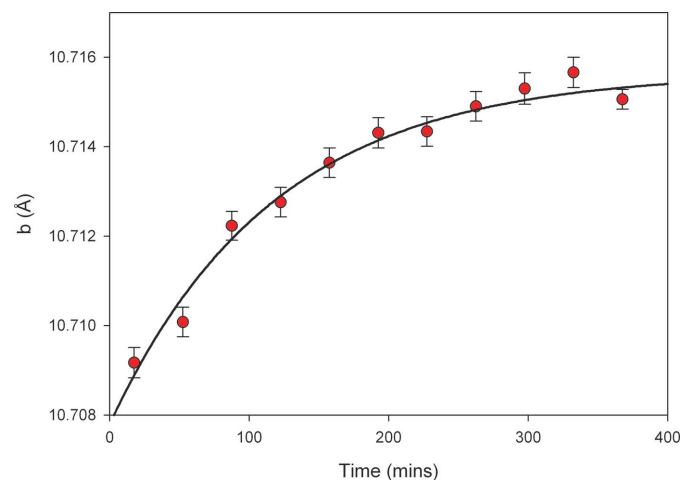


Figure 7 Variation of the *b* lattice constant of β -sulfur at 125 K as a function of time. The solid line is a least-squares fit to the data using the function $b = b_\infty - \Delta b \exp(-t/\tau)$ to model the thermal equilibration of the sample. The characteristic time $\tau = 117$ (11) min, $b_\infty = 10.7157$ (1) Å and $\Delta b = 0.0077$ (4) Å.

Table 3

Thermal conductivity values of the experimental components.

| | λ (W cm ⁻¹ K) ⁻¹ |
|-----------|--|
| Sulfur | 0.003 |
| Aluminium | 2.370 |
| Vanadium | 0.307 |
| (Sawdust) | (0.001) |

the *a* axis (Fig. 2) there is a sheet of S₈ type (I) molecules followed by a sheet of type (II) molecules; the sheets are rotated, relative to the axis, by -45 and $+45^\circ$, respectively. The sheet of type (III) molecules is thus required to rotate in both senses, which is achieved through the disorder.

Detailed analysis of the variation of lattice constants as a function of temperature can provide valuable information, especially with the high precision obtained by high-resolution neutron powder diffraction. A number of different functions, derived from the analysis of heat-capacity data, can be used to model the normal variation of the lattice parameters from which any residual variation can be obtained (David *et al.*, 1993). However, such a detailed analysis has not been possible with the present data for the following reasons.

Inspection of the lattice-constant data shown in Fig. 6 outside the region of the phase transition shows discontinuities every 25 K. The 25 K breaks correspond to temperatures at which the data-collection time was longer, thus revealing the exceptionally slow attainment of thermal equilibrium of the sample. The unit-cell volume can be fitted successfully to a simple quadratic function (Fig. 6c) using the points corresponding to the long count-time data. Using the quadratic parameterization the expansion coefficient at 100 and 175 K is calculated as 5.50×10^{-6} and 4.45×10^{-6} K⁻¹, respectively. These values are significantly lower than those reported for orthorhombic sulfur in the α phase (23.5×10^{-6} K⁻¹ at 98 K, 112×10^{-6} K⁻¹ at 173 K) based on X-ray powder diffraction data (Wallis *et al.*, 1986).

In a separate experiment, data were recorded on a second sample at fixed temperature (125 K) at intervals of 25 min, the sample having followed a temperature ramp from 100 K as in the first experiment. Variation of the lattice parameter as a function of time is shown in Fig. 7. An exponential increase with time was observed in all the lattice constant values that can be well fitted with an average characteristic time of $\tau = 117$ (11) min. Selected values of thermal conductivity (Weast, 1986) for the sample-can component materials are listed in Table 3. The figures highlight the good insulating properties of elemental sulfur, which most likely accounts for the anomalous lattice constant behaviour. Nevertheless, the possibility of a relaxation of the structure on warming, especially in view of the intrinsic disorder and method of formation of the sample, cannot be discounted. These effects and the observed saturation effects of the critical behaviour and the likely premonitory effects observed in the lattice constants all require an improved experimental set-up before a more

detailed analysis can be undertaken. A new design of sample can is required to circumvent the problems owing to the very low thermal conductivity of elemental sulfur and to allow better thermal contact between the powder, sensor and heater.

4. Conclusions

The anticipated advantage of the present powder study over the 30-year old single-crystal X-ray study was the increased number of temperatures at which the disordered site occupancy could be determined. Although this was the case, the need to spend more time both to improve counting statistics and to achieve thermal equilibrium ultimately reduced the precision to which the dimensionality of the transition could be determined. It should be noted that the issue of sample temperature equilibrium is rarely a problem with neutron powder diffraction, although with the ever-reducing counting times expected from diffractometers on the new high-flux spallation neutron sources due on-line in the next few years, it is one that should not be forgotten. The precision afforded by single-crystal studies is hard to match even with high-resolution powder data and observations of diffuse scattering associated with the transition cannot be reproduced in a powder study. It should also be recognized that by utilizing modern synchrotron sources, a much more complete single-crystal experiment can be carried out today than was possible at the time of the Goldsmith and Strouse study. In this case, however, concerns regarding thermal equilibrium may well be replaced by problems associated with beam heating and radiation damage to the crystal. Indeed in a recent synchrotron powder experiment by the present authors on the ID31 beamline at the European Synchrotron Radiation Facility, anomalous lattice-parameter behaviour attributable to radiation damage was observed in a sample of α -sulfur at ambient temperature during a 30 minute exposure period using a $\lambda = 0.802$ Å beam.

In summary, high-resolution neutron powder diffraction has been used to characterize the order–disorder transition in monoclinic cyclo-octasulphur. Despite the structural complexity and low thermal conductivity of the sample, a constant, rapid data-collection strategy combined with the novel use of geometrically constrained refinements has allowed the direct and precise determination of the order parameter to be obtained from the analysis of molecular site occupancies. The transition is critical and continuous with a transition temperature, $T_c = 198.4$ (3) K, and a critical exponent, $\beta = 0.28$ (3), indicative of three-dimensional ordering controlled by van der Waals interactions.

This work has been supported by CCLRC with the provision of neutron beam time.

References

- Collins, M. F. (1989). *Magnetic Critical Scattering. Oxford Series on Neutron Scattering in Condensed Matter*. New York, USA: Oxford University Press Inc.

- Coppens, P., Yang, Y. W., Blessing, R. H., Cooper, W. F. & Larsen, F. K. (1977). *J. Am. Chem. Soc.* **99**, 760–766.
- David, W. I. F., Ibberson, R. M. & Matsuo, T. (1993). *Proc. R. Soc. Lond. A*, **442**, 129–146.
- David, W. I. F., Ibberson, R. M. & Matthewman, J. C. (1992). Rutherford Appleton Laboratory Report, RAL-92-032.
- Donahue, J. (1982). *The Structure of the Elements*. Malabar, Florida: Krieger Publishing Company.
- Goldsmith, L. M. & Strouse, C. E. (1977). *J. Am. Chem. Soc.* **99**, 7580–7589.
- Ibberson, R. M., David, W. I. F. & Knight, K. S. (1992). Report RAL-92-031. Rutherford Appleton Laboratory, Chilton, Didcot, England.
- Meyer, B. (1976). *Chem. Rev.* **76**, 367–388.
- Montgomery, R. L. (1974). *Science*, **184**, 562–563.
- Muto, T. & Takagi, Y. (1955). *The Theory of Order–Disorder Transitions in Alloys*. Solid State Reprints. New York: Academic Press.
- Pawley, G. S. & Rinaldi, R. P. (1972). *Acta Cryst.* **B28**, 3605–3609.
- Pastorino, C. & Gamba, Z. (2001). *J. Chem. Phys.* **115**, 9421–9426.
- Pastorino, C. & Gamba, Z. (2003). *J. Chem. Phys.* **119**, 2147–2154.
- Rettig, S. J. & Trotter, J. (1987). *Acta Cryst.* **C43**, 2260–2262.
- Sands, D. E. (1965). *J. Am. Chem. Soc.* **87**, 1395–1396.
- Spek, A. L. (2003). *J. Appl. Cryst.* **36**, 7–13.
- Templeton, L. K., Templeton, D. H. & Zalkin, A. (1976). *Inorg. Chem.* **15**, 1999–2001.
- Wallis, J., Sigalas, I. & Hart, S. (1986). *J. Appl. Cryst.* **19**, 273–274.
- Weast, R. C. (1986). Editor. *CRC Handbook of Chemistry and Physics*. Boca Raton, Florida: CRC Press, Inc.